



Cite this: *Biomater. Sci.*, 2018, **6**, 3075

A modular assembly pH-sensitive charge reversal siRNA delivery system†

Qiong Sun, Chunming Tang, Zhigui Su, Junjie Du, Yunkai Shang, Lingjing Xue and Can Zhang *

Cationic lipids and polymers are the most common non-viral vectors for siRNA delivery; however, their intense positively charged character may give rise to serum-triggered aggregation, immune activation, inflammation stimulation and grievous toxicity. An ocean of charge shielding strategies is exploited, but the currently available siRNA delivery systems still remain ungratified and deficient. Herein, we developed a facile modular assembly strategy for a pH-sensitive charge reversal siRNA delivery system (PC), which can be easily obtained by adjusting the ratios of positively and negatively charged modules. This PC is electronegative at neutral pH and reverses to electropositive at an acidic pH value with increased tumor cellular uptake. Also, the PC can promote efficient intracellular release and cytoplasmic distribution of siRNA, due to its fusogenic potential with the lysosome membrane. Moreover, the PC loaded with siRNA targeting survivin mRNA (cpusiRNA2) specifically down-regulated the expression of survivin, possessing remarkable tumor therapeutic efficacy *in vitro* and *in vivo*. Accordingly, this handy and effective assembly strategy would provide a promising platform for the design of siRNA delivery systems in cancer therapy.

Received 1st September 2018,
Accepted 28th September 2018

DOI: 10.1039/c8bm01062e

rs.c.li/biomaterials-science

1. Introduction

Small interfering RNA (siRNA) has been proved to be a potential therapeutic candidate for numerous diseases, owing to its eminent gene-silencing capacity.^{1–4} However, the clinical application of siRNA is overwhelmingly impeded by its innate limitations such as labile enzymatic digestion in blood, rapid renal clearance and restricted cytoplasmic membrane penetrability.⁵ Accordingly, safe and effective delivery systems are indispensable for the therapeutic implementation of siRNA.^{6–9} Cationic lipids and polymers, the most quintessential non-viral vectors for siRNA delivery, can assemble efficiently with siRNA to form a complex with reinforced cellular uptake and satisfactory gene-silencing efficiency.^{10–13} Nevertheless, the strong positive surface charge related to these complexes may give rise to serum-triggered aggregation, immune activation, inflammation stimulation and grievous toxicity.¹⁴ Consequently, a plethora of charge shielding strategies are exploited to settle these arduous problems associated with the cationic property of siRNA delivery systems.^{15–17} The methods to bring down the surplus positive charge can be mainly classified into two cat-

egories. One is reducing the positive charge density of the vectors by decoration with poly(ethylene glycol) (PEG) or poly-anions.^{18,19} However, the steric hindrance of the incorporated PEG chain or polyanions hampers the uptake by tumor cells. The other is introducing sheddable coatings to the surface of cationic vector/siRNA complexes, such as tumor acidity-sensitive covalent linkage of PEG,²⁰ enzyme-responsive polyanion,²¹ or charge reversal polymer which is negatively charged in the blood circulation, while reversing to positive charge in the acidic tumor microenvironment resulting in the detachment from the complex caused by electrostatic repulsion.²² Despite the promoted cellular uptake of siRNA delivery systems utilizing these effective strategies, the dilemma in the labile and charge reversal materials of the microenvironment still needs to be addressed.

Herein, we developed a convenient assembly strategy for charge reversal siRNA delivery, which has a particular isoelectric point *via* adjusting the ratios of positively and negatively charged modules. Specifically, the cationic lipid LG2C₁₄ and its azido-bearing derivative N₃-LG2C₁₄ were regarded as electropositive blocks, while propionic acid (PA) was taken as an electronegative block, as well as anionic siRNA. Firstly, the electropositive modules, LG2C₁₄ and N₃-LG2C₁₄, together with a natural soy phosphatidylcholine (SPC) and cholesterol are used to prepare a functionalized cationic liposome (N₃-CL). Then, this cationic liposome N₃-CL combined with the electronegative module siRNA to form an azido-functionalized complex N₃-CL/siRNA *via* electrostatic interaction. Finally, the electronegative module PA with an alkynyl group and the

State Key Laboratory of Natural Medicines and Jiangsu Key Laboratory of Drug Discovery for Metabolic Diseases, Center of Advanced Pharmaceuticals and Biomaterials, China Pharmaceutical University, Nanjing 210009, China.

E-mail: zhangcan@cpu.edu.cn

† Electronic supplementary information (ESI) available. See DOI: 10.1039/c8bm01062e

azido-functionalized complex N_3 -CL/siRNA were assembled into a pH-sensitive charge reversal siRNA delivery system (PC) based on the covalent binding of the alkyne and azido groups. As illustrated in Fig. 1, the PC is expected to have good colloidal stability and preferentially accumulates at the tumor site after intravenous administration. Owing to sufficient PA module, the negative surface charge of the PC under neutral pH conditions reduces the nonspecific interactions with serum proteins during blood circulation (pH 7.4) and significantly improves

their accumulation in the tumor tissue (pH 6.5). When the PC arrives at the acidic tumor tissue *via* the enhanced permeability and retention (EPR) effect,²³ its surface charge reverses to positive due to the protonation of electronegative PA module and electropositive N_3 -LG2C₁₄ module, thus promoting efficient tumor cellular uptake. Subsequent entering into the more acidic endosome/lysosome environment (pH 5.5) will cause protonation of the amino groups on the surface of the complex, which can bring about a stronger positive charge, hence forming an ion pair between the cationic lipids in the complex and the anionic lipids of the endosome membrane. Consequently, the disassembly of the complex takes place on account of the fusion of the lipids and endosome membrane, leading to the release of siRNA into the cytoplasm and finally enhancement of the RNA-interfering effect. This modular assembly strategy may provide a splendid charge shielding means and constitute a promising platform for the design of targeting siRNA delivery systems in the therapeutic intervention of malignant tumors.

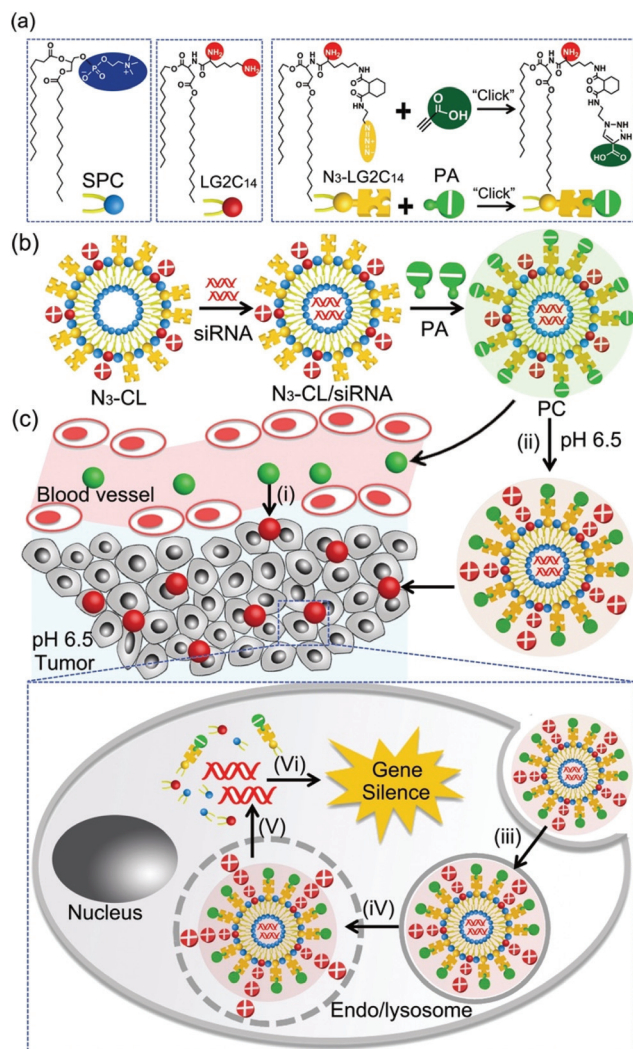


Fig. 1 (a) Different modules with various structures and functionalities. (b) Construction of the modular assembly pH-sensitive charge reversal complex (PC) for siRNA delivery. (c) Schematic representation of siRNA systemic delivery by means of the PC. (i) Accumulation of the negatively charged PC in the tumor tissues *via* the enhanced permeability and retention (EPR) effect; (ii) charge reversal of the PC in the acidic tumor microenvironment; (iii) enhanced tumor cellular uptake due to the cationic characteristic of the PC; (iv) the stronger positively charged PC in the more acidic endosome/lysosome, owing to the protonation of amino groups on the surface of the complex; (v) siRNA release in the cytoplasm on account of the fusion of cationic lipids and the endosome membrane; (vi) the RNA-interfering effect and gene silencing.

2. Experimental

2.1 Materials

Di-*tert*-butoxycarbonyl-L-lysine (Boc-L-Lys(Boc)-OH), L-glutamic acid and *N*-benzyloxycarbonyl-*N'*-(*tert*-butoxycarbonyl)-L-lysine (Boc-L-Lys(Z)-OH) were purchased from GL Biochem Co. Ltd (Shanghai, China). Rhodamine B isothiocyanate was obtained from Life Technology. Bathophenanthroline disulfonic acid disodium salt hydrate (ligand) was supplied by Tokyo Chemical Industry Co., Ltd (Shanghai, China). Sodium azide was obtained from Tianzun Zezhong Chemical Co. Ltd (Nanjing, China). Soya bean lecithin (SPC) was provided by Toshisun Biology & Technology Co. Ltd. Goldview, agarose, 6× sucrose DNA loading buffer and trypsin were provided by Sunshine Biotechnology Co., Ltd (Nanjing, China). LysoTracker Red, RIPA lysis buffer, phenylmethanesulfonyl fluoride (PMSF), Bradford Protein Assay Kit, Annexin V-FITC Apoptosis Detection Kit and Cell Cycle and Apoptosis analysis kit were purchased from Beyotime Institute of Biotechnology (Nantong, China). BCA protein assay kit was obtained from TIANGEN Biotech Co., Ltd (Beijing, China). Lysosomal isolation kit was purchased from GENMED Biotechnology Co., Ltd (Shanghai, China). Fluorescently labeled siRNA (FAM-siRNA), the negative control siRNA (siN.C.), the primers used in the qRT-PCR for survivin and GAPDH (survivin-forward: 5'-CGACGTTGCCCTGCCTG-3', survivin reverse 5'-AAGGAAAGCGCAACCGGAC-3', GAPDH forward: 5'-TTCACCACCATGGAGAAGGC-3', GAPDH reverse: 5'-GGCATGGACTGTGGTCATGA-3') and 2× SYBR Green qPCR Mix were obtained from Baiao Biotechnology Co., Ltd (Nantong, China). Cy5-labeled scrambled siRNA (Cy5-siRNA), siRNA targeting survivin mRNA (cpusirna2, sense siRNA strand: 5'-GAAUUUGAGGA AACUGCGAtt-3', antisense siRNA strand: 3'-ttCUAAACUCCUUUGACGCU-5') was supplied by Tao Xi's group (China Pharmaceutical University, China). All

other chemicals were obtained from Aladdin Reagent Inc. (Shanghai, China).

2.2 Modular assembly and characterization

Cationic liposomes and azide functionalized cationic liposomes were prepared by a thin-film dispersion method. SPC (20 mg), LG2C₁₄ (10 mg), N₃-LG2C₁₄ (10 mg) and cholesterol (12 mg) were dissolved in 5 mL of the mixture of CHCl₃ and MeOH (3 : 2, v : v). After the organic solvents were removed by rotary evaporation at 40 °C, the thin lipid film formed was further dried under vacuum overnight to remove any traces of the remaining solvents. Subsequently, the lipid film was hydrated in 5 mL of distilled water at 37 °C. N₃-CL was dispersed by using an ultrasonic cell disruptor (Lifecientz Biotech Co. Ltd, China), and then extruded repeatedly through polycarbonate membrane filters with a pore size of 0.22 μm. As a control, the cationic liposome CL without an azide group was also prepared containing SPC (20 mg), LG2C₁₄ (20 mg) and cholesterol (12 mg) by a similar method. 9.5 μL of N₃-CL (10.4 mg mL⁻¹) was gently mixed with 12 μL of cpusirRNA2 (0.5 mg mL⁻¹) to obtain the complex N₃-CL/cpusirRNA2 after incubation for 20 min at room temperature. Then, N₃-CL/cpusirRNA2 was added into the mixed solution containing 13.2 μL of propionic acid (PA) (1.132 μg μL⁻¹), 4.2 μL of sodium ascorbate (1 mg mL⁻¹), 5 μL of CuSO₄ (0.1 mg mL⁻¹) and 2.3 μL of copper ion–ligand (L) (1 mg mL⁻¹) under stirring at room temperature for 30 min to obtain the pH-sensitive charge-reversal complex (PC) after the removal of the catalysts by using centrifugal filter devices (10 K MWCO) (Millipore).

For the preparation of the cationic complex (CC), 6.5 μL of CL (10.4 mg mL⁻¹) was gently mixed with 12 μL of cpusirRNA2 (0.5 mg mL⁻¹) with incubation for 20 min at room temperature. The particle size and zeta potential were measured by using a dynamic light scattering (DLS) analyzer and a ZetaPlus zeta potential analyzer (Brookhaven), respectively. The morphology of the PC was characterized using a high resolution transmission electron microscope (HRTEM) with an operating voltage of 200 kV (JEM-2100F, Hitachi). Fourier-transform infrared (FTIR) measurements of N₃-CL/cpusirRNA2 (5 mg) and the PC (5 mg) were performed on a Nicolet 55xc FTIR spectrometer by preparing KBr pellets. For the UV-vis absorption assay, 2 mL of the solution of PA (7.5 μg mL⁻¹), N₃-CL/siRNA (52.4 μg mL⁻¹), N₃-CL/siRNA + PA (52.4 μg mL⁻¹ + 7.5 μg mL⁻¹) and the PC (53.2 μg mL⁻¹) were detected on a UV/Visible spectrophotometer (EU-2600A). For the gel retardation assay, 20 μL of N₃-CL/cpusirRNA2 and the PC containing 2 μg cpusirRNA2 at different N : P ratios (0, 0.5, 1, 2, 3, 4) were gently mixed with 4 μL of 6× DNA loading buffer and subjected to agarose gel electrophoresis (1%) with 5% Goldview. The electrophoresis was carried out at a voltage of 130 V for 15 min in Tris-acetate-EDTA (TAE) buffer.

2.3 Evaluation of the *in vitro* stability

The variation in the particle size of the PC was monitored in the presence of fetal blood serum (FBS) and at different pH values (pH 7.4 and 6.5). Briefly, 300 μL of the PC (0.35

mg mL⁻¹) was diluted with 3 mL of HEPES buffer solution (20 mM, pH 7.4), acetate buffer solution (20 mM, pH 6.5) or Dulbecco's modified Eagle's medium (DMEM) (Hyclone) with 10% (v : v) FBS. After incubation for prearranged time intervals, the particle size was measured. The CC carrying 6 μg cpusirRNA2 was treated as a control.

Meanwhile, the stability of the PC under different surroundings was further determined by taking advantage of fluorescence resonance energy transfer (FRET) analysis. 200 μL of the double-fluorescence labeling PC containing RhB-N₃-LG2C₁₄ (6 μg) and FAM-labeled siRNA (6 μg) was added into 2.7 mL of HEPES buffer solution (20 mM, pH 7.4), acetate buffer solution (20 mM, pH 6.5) or DMEM with 10% FBS for prearranged time intervals (0, 2, 4, 6, 8, 12 h) at 37 °C. After incubation, fluorescence intensities were determined by using a fluorescence spectrophotometer. According to the following equation:²⁴

$$\text{FRET ratio} = I_{\text{RhB}} / (I_{\text{RhB}} + I_{\text{FAM}}) \times 100\%$$

FRET efficiency (FRET ratio) can be calculated by measuring the fluorescence intensities of RhB at 575 nm and FAM at 525 nm, respectively.

To investigate the protection of cpusirRNA2 by the PC against RNase A, the PC loaded with cpusirRNA2 (2 μg) at different N : P ratios was incubated with RNase A (2 μL, 5 U μL⁻¹) at 37 °C for 30 min. 5 μL of sodium dodecyl sulfate (SDS) (2%) was added to extract cpusirRNA2 from the PC.

2.4 Fusion assay of the PC with the lysosome membrane

The membrane fusion between the PC and lysosome membrane was investigated to explore the disassembly mechanism of the prepared PC carrying 6 μg cpusirRNA2 by using a fluorescence resonance energy transfer (FRET) assay. The constructed PC was labeled with RhB-N₃-LG2C₁₄ and *N*-(7-nitrobenz-2-oxa-1,3-diazol-4-yl)-phosphatidylethanolamine (NBD-PE), whose concentrations were 1 mol%. The isolation of lysosomes was carried out according to the guide of the lysosomal isolation kit. In brief, Bel-7402 cells amounting to 1 × 10⁸ cells were resuspended in 10 mL of cleaning reagent A (provided in the kit) and then centrifuged at 300g for 10 min. After removing the supernatant, 5 mL of a cold lysis solution was added into the cells and the cell lysates were incubated on ice for 2 min, and vortexed every 5 seconds. Then, 5 mL of preservation solution F was mixed, followed by 500 μL of cold enhanced Reagent D. Subsequently, the mixed solution was centrifuged at 1500g at 4 °C for 10 min in order to remove the nuclei and intact cells; then the supernatant was centrifuged at 3000g at 4 °C for 10 min. The isolated solution was added into the supernatant, and incubated on ice for 15 min. The supernatant was centrifuged at 25 000g at 4 °C for 20 min in order to obtain the lysosomes. After removing the supernatant, 500 μL of preservation solution F was added to dissolve the lysosomes, which were store at -70 °C.

For the fusion assay, the double-labeled PC with 6 μg cpusirRNA2 was incubated with 165 μL of isolated lysosomes (0.6 mg mL⁻¹) in the buffer solution with different pH values (pH 7.4, pH 6.5, pH 5.5, pH 4.5) at 37 °C for a preset period of

time. Fluorescence intensity was determined at an excitation wavelength of 460 nm and an emission wavelength of 530 nm. The percentage of lipid mixing between the lysosome membrane and the cationic assemblies over time was calculated using the following equation:²⁵

$$\text{Lipid mixing (100\%)} = (F_t - F_0)/(F_{\text{TX}} - F_0) \times 100\%$$

where F_t is the fluorescence intensity at preset time intervals, F_0 is the primary fluorescence intensity, and F_{TX} is the fluorescence intensity after the addition of Triton X-100 to destroy the PC.

2.5 Cell culture

Human hepatocellular carcinoma cells (Bel-7402) were cultured in DMEM with 10% FBS, 100 U mL⁻¹ penicillin and 100 mg mL⁻¹ streptomycin at 37 °C under an atmosphere of 5% CO₂ and 90% relative humidity. Human hepatic L02 cells were maintained in RPMI-1640 medium containing 10% FBS, 100 U mL⁻¹ penicillin and 100 mg mL⁻¹ streptomycin at 37 °C in a 5% CO₂ incubator. The cells were subcultured approximately every 3 days at 80% confluence using 0.25% (w:v) trypsin at a split ratio of 1 : 5.

2.6 Cellular uptake

Bel-7402 cells (1×10^5 cells per well) were seeded into 24-well plates in 0.5 mL of complete DMEM medium (supplemented with 10% FBS and 1% antibiotics) and cultured at 37 °C under a 5% CO₂ humidified atmosphere for 24 h. The medium was replaced with fresh DMEM medium without FBS and antibiotics. After 4 h, the cells were incubated with 0.5 mL of fresh DMEM medium (pH 7.4 or 6.5) containing the PC or CC loaded with FAM-siRNA (200 nM). After 3 h, the cells were washed with cold PBS thrice and trypsinized. Trypsinization was stopped by adding 4 °C complete culture medium. After centrifugation, the cells were washed twice with 4 °C PBS. Finally, the cell suspension in PBS was filtered through 35 μm nylon mesh and subjected to flow cytometric analysis using a flow cytometer (BD FACSCalibur).

For confocal laser scanning microscopy (CLSM) observation, Bel-7402 cells (1×10^5 cells per well) were seeded into special confocal microscopy dishes and incubated for 24 h. The medium was replaced with 0.5 mL of fresh DMEM medium without FBS and antibiotics. After 4 h, the cells were incubated with 0.5 mL of fresh DMEM medium (pH 7.4 or 6.5) containing the PC or CC, and loaded with FAM-siRNA (200 nM). After 3 h, the cells were washed with PBS thrice and observed by CLSM.

In order to determine the cellular internalization pathways of the PC, Bel-7402 cells were first incubated with different specific agents for various kinds of endocytosis (inhibitor of clathrin-mediated endocytosis: chlorpromazine²⁶ (20 μg mL⁻¹); inhibitor of caveolin-mediated endocytosis: nystatin²⁷ (15 μg mL⁻¹); inhibitor of macropinocytosis: amiloride²⁸ (133 μg mL⁻¹) and inhibitor of energy-dependent sodium azide²⁹ (1 mg mL⁻¹)) for 1 h at 37 °C. Subsequently, the medium was replaced with 0.5 mL of the PC loaded with FAM-

siRNA (200 nM) at 37 °C. After 3 h, the cells were washed with cold PBS thrice and trypsinized. Trypsinization was stopped by adding 4 °C complete culture medium. After centrifugation, the cells were washed twice with 4 °C PBS. Finally, the cell suspension in PBS was filtered through 35 μm nylon mesh and subjected to flow cytometric analysis using a flow cytometer (BD FACSCalibur).

To observe and study the uptake kinetics of the PC, Bel-7402 cells were incubated with 0.5 mL of the PC at a FAM-siRNA concentration of 200 nM for prearranged time intervals (0, 0.5, 1, 2, 3 and 4 h) or with the PC at different concentrations of FAM-siRNA for 3 h at 37 °C. Subsequently, the cells were washed with cold PBS thrice and trypsinized. Trypsinization was stopped by adding 4 °C complete culture medium. After centrifugation, the cells were washed twice with 4 °C PBS. Finally, the cell suspension in PBS was filtered through 35 μm nylon mesh and subjected to flow cytometric analysis using a flow cytometer (BD FACSCalibur).

2.7 Intracellular distribution and siRNA release

The intracellular delivery of the PC in Bel-7402 cells was evaluated by CLSM. The localization of the PC loaded with FAM-siRNA was visualized by labeling endosomes/lysosome with LysoTracker Red. The cells (1×10^5 cells per well) were seeded in special confocal microscopy dishes for 24 h at 37 °C, followed by cell incubation with 0.5 mL of the PC loaded with FAM-siRNA (200 nM) for prearranged time intervals (3 h and 6 h). Subsequently, the cells were washed with cold PBS thrice and incubated with 250 nM LysoTracker Red for 30 min at 37 °C. Finally, the cells were washed with PBS thrice and observed by CLSM.

In order to observe the disassembly of the PC loaded with FAM-siRNA, the cationic liposome was labeled with RhB-N₃-LG2C₁₄ (5.7 w/w% of the total lipids). The cells (1×10^5 cells per well) were seeded in special confocal microscopy dishes for 24 h at 37 °C, followed by cell incubation with 0.5 mL of the RhB-labeled PC loaded with FAM-siRNA (200 nM) for prearranged time intervals (3 h and 6 h). Subsequently, the cells were washed with cold PBS thrice and observed by CLSM.

2.8 Survivin gene silencing and cell apoptosis

Bel-7402 cells were seeded into 6-well plates at 4×10^5 cells per well in 2 mL of complete DMEM medium and cultured at 37 °C under a 5% CO₂ humidified atmosphere for 24 h. The medium was replaced with 2 mL of fresh DMEM medium without FBS and antibiotics. After 4 h, the cells were incubated with 2 mL of fresh DMEM medium (pH 7.4 or 6.5) containing the PC or CC, loaded with 200 nM cpusRNA2 or siN.C. After 3 h, the culture medium was replaced with 2 mL of fresh complete DMEM medium (supplemented with 10% FBS and 1% antibiotics) with further incubation for 48 h at 37 °C. The cellular levels of survivin mRNA and protein were assessed using quantitative real-time PCR (qRT-PCR) and western blot analysis, respectively.

For qRT-PCR analysis, the cells were collected and total RNA from the transfected cells was isolated using TRIzol

Reagent (Life Technologies) according to the protocol of the manufacturer. 2 μg of total RNA was transcribed into cDNA using the PrimeScript 1st Strand cDNA Synthesis Kit (Takara, Dalian, China). Then, 2 μL of cDNA, 10 μL of 2 \times SYBR Green qPCR Mix, 6 μL of DPEC water, 1 μL of the forward primer (10 μM) and 1 μL of the reverse primer (10 μM) for survivin or glyceraldehyde 3-phosphate dehydrogenase (GADPH) were mixed together and subjected to qRT-PCR analysis (StepOne™ System, USA).

For western blot analysis, the cells were collected and then resuspended in 100 μL of RIPA lysis buffer supplemented with 1% phenylmethanesulfonyl fluoride (PMSF). The cell lysates were incubated on ice for 0.5 h and vortexed every 5 min. The lysates were then clarified by centrifugation at 4 °C at 12 000g for 10 min. The protein concentration was determined using the BCA protein assay kit (Thermo Scientific). Total protein (150 μg) was separated on 15% bis-Tris-polyacrylamide gel and then transferred (at 200 mA for 1 h) to PVDF membranes (Millipore). After incubation in 5% milk in Tris buffered saline Tween-20 (TBST, pH 7.5) at 37 °C for 1 h, the membranes were incubated in 0.5% BSA in TBST with survivin rabbit monoclonal antibody (1 : 1000) and anti- β -actin mouse monoclonal antibody (1 : 500) overnight. After incubation in 5% milk with goat anti-rabbit IgG/HRP (1 : 5000) and goat polyclonal secondary antibody to mouse IgG/HRP (1 : 10 000) for 30 min, protein bands were visualized by using an enhanced chemiluminescent substrate (Beyotime, China).

For the analysis of cell apoptosis, Bel-7402 cells were seeded into 12-well plates at 2×10^5 cells per well in 1.0 mL of complete DMEM medium and cultured at 37 °C under a 5% CO₂ humidified atmosphere for 24 h. The medium was replaced with 1 mL of fresh DMEM medium without FBS and antibiotics. After 4 h, the cells were incubated with 1 mL of fresh DMEM medium (pH 7.4 or 6.5) containing the PC or CC, loaded with 200 nM cpusirRNA2 or siN.C. After 3 h, the culture medium was replaced with 1 mL of fresh complete DMEM medium (supplemented with 10% FBS and 1% antibiotics) with further incubation for 48 h at 37 °C. Then, the cells were washed with cold PBS thrice and trypsinized. Trypsinization was stopped by adding 4 °C complete culture medium. After centrifugation, the cells were suspended in the 1 \times binding buffer, followed by washing twice with 4 °C PBS. 5 μL of Annexin V-FITC was added into the cell suspensions for 15 min of incubation, and then 5 μL of propidium iodide (PI) was added. The cells were immediately analyzed by flow cytometry.

L02 cells were seeded into 12-well plates at 1.5×10^5 cells per well in 1.0 mL of complete RPMI medium 1640 and cultured at 37 °C under a 5% CO₂ humidified atmosphere for 24 h. The medium was replaced with 1 mL of fresh RPMI medium 1640 without FBS and antibiotics. After 4 h, the cells were incubated with 1 mL of fresh RPMI medium 1640 containing the PC or CC, loaded with 200 nM cpusirRNA2. After 3 h, the culture medium was replaced with 1 mL of fresh complete RPMI medium 1640 (supplemented with 10% FBS and 1% antibiotics) with further incubation for 48 h at 37 °C. The next procedures were the same as those for the Bel-7402 cells.

2.9 Inhibitory effect against L02 cells

An MTT assay was used to measure cell proliferation and viability. Briefly, L02 cells (5×10^3 cells per well) were plated in 96-well plates and routinely cultured for 24 h. The medium was replaced with fresh RPMI medium 1640 without FBS and antibiotics. After 4 h, the cells were treated with various concentrations of cpusirRNA2 (100, 150, 200, 250, 300, 400 nM) encapsulated in the CC and PC in RPMI medium 1640. After 3 h, the medium was removed and the cells were washed with cold PBS twice, followed by the addition of complete RPMI medium and incubation for another 48 h. The medium was removed and 20 μL MTT solution (5 mg ml⁻¹) was added to each well, followed by incubation for 4 h at 37 °C under 5% CO₂. The MTT solution was removed, and 150 μL DMSO was added to each well to dissolve the blue MTT formazan crystal that had formed. Absorbance was measured at 570 nm using a microplate reader. All experiments were performed in quadruplicate.

2.10 Cell cycle assay

L02 cells were seeded into 12-well plates at 1.5×10^5 cells per well in 1.0 mL of complete RPMI medium 1640 and cultured at 37 °C under a 5% CO₂ humidified atmosphere for 24 h. The medium was replaced with 1 mL of fresh DMEM medium without FBS and antibiotics. After 4 h, the cells were incubated with 1 mL of fresh RPMI medium 1640 containing the PC or CC, loaded with 200 nM cpusirRNA2. After 3 h, the culture medium was replaced with 1 mL of fresh complete RPMI medium 1640 (supplemented with 10% FBS and 1% antibiotics) with further incubation for 48 h at 37 °C. Then, the cells were washed with cold PBS thrice and trypsinized. The cells (1×10^6) were collected by centrifugation at 1000g for 5 min, washed twice with ice cold PBS, and then fixed with 70% cold ethanol and stored at 4 °C for 24 h. After fixation, the cells were centrifuged again, washed with cold PBS twice, and stained with 0.5 ml of propidium iodide (PI) staining buffer, which contains 200 mg ml⁻¹ RNase A and 50 μg ml⁻¹ PI, at 37 °C for 30 min in the dark. The cell cycles were analyzed using a flow cytometer at 488 nm, and the percentage of cells in each phase of the cell cycle was evaluated.

2.11 Animals and tumor xenograft models

Male ICR mice (18–22 g) were bought from the College of Veterinary Medicine, Yangzhou University (Jiangsu, China). All the animal experiments were performed in compliance with the Guide for Care and Use of Laboratory Animals, approved by China Pharmaceutical University.

For the establishment of tumor xenograft models, the male ICR mice were subcutaneously inoculated with 1×10^6 mice hepatocellular carcinoma (Heps) cells suspended in 200 μL of saline. The length (L) and width (W) of the tumor were determined by using a Vernier caliper. The tumor volume (V) was calculated according to the equation:

$$V = L \times W^2 / 2$$

2.12 *In vivo* biodistribution

When the tumor volume reached about 300 mm³, the mice were intravenously injected with naked Cy5-siRNA, and CC and PC loaded with Cy5-siRNA at a dose of 1 mg kg⁻¹. After injection, the images of the tumor-bearing mice were acquired at different time intervals on an *in vivo* Maestro™ imaging system (Cambridge Research & Instrumentation, USA). At 24 h post-injection, the mice were sacrificed. The tumor and normal tissues (heart, liver, spleen, lung, kidney) were harvested for *ex vivo* imaging, and the region-of-interest (ROI) analysis was performed. The tumor section was also obtained for the observation of the intratumoral distribution with the cell nuclei stained with Hoechst 33258 (1 μg mL⁻¹) for 5 min at room temperature. The tumor sections were observed using CLSM.

2.13 Therapeutic efficiency

Therapeutic efficiency was assessed using ICR mice bearing mice hepatocellular carcinoma (Heps) xenograft tumors. When the tumor reached about 25 mm³, the Heps tumor-bearing ICR mice were intravenously injected with (1) saline; (2) naked cpusRNA2; (3) PC/siRNA and (4) CC or PC loaded with cpusRNA2 at a dose of 1.2 mg kg⁻¹ every other day (0, 2, 4, 6 and 8 days). The body weight and the tumor size were measured during the treatment. At day 10, the mice were sacrificed. The tumors were harvested and weighed. The tumor index was calculated as the weight ratio of the tumor to the body. For histological analysis, paraffin sections of the tumor were stained with hematoxylin and eosin (HE) and visualized by using an inverted fluorescence microscope (FV1100, Olympus). Moreover, the survival rates were also monitored.

2.14 Caspase-3 activity assay

The healthy ICR mice were intravenously injected with (1) saline and (2) CC or PC loaded with cpusRNA2 at a dose of 1.2 mg kg⁻¹ every other day (0, 2, 4, 6 and 8 days). At day 10, the mice were sacrificed. The livers, spleens, lungs and kidneys were harvested and used for experiments. The activities of caspase-3 were measured using a commercialized caspase-3 activity kit (Beyotime, China). In brief, the livers, spleens, lungs and kidneys were homogenized in a lysis buffer. The lysate was centrifuged at 20 000g for 15 min at 4 °C, and the supernatants were incubated for 2 h at 37 °C with 10 μL caspase-3 substrate (Ac-DEVDpNA) (2 mM). Substrate cleavage was measured with a spectrofluorometer at 405 nm.

3. Results and discussion

3.1 Modular assembly and characterization of the pH-sensitive charge-reversal complex (PC)

Firstly, we synthesized the amino-acid-based cationic lipid blocks, LG2C₁₄ (Scheme S1†) and its azido-bearing derivative N₃-LG2C₁₄ (Scheme S2†), and prepared the azide functionalized cationic liposomes (N₃-CL) using the thin-film dispersion method. Then, the N₃-CL/siRNA complex was assembled based

on the electrostatic interaction between the cationic liposomes N₃-CL and siRNA at various molar ratios of nitrogen in the cationic liposomes to phosphate in siRNA (N/P ratio). The azide-functionalized complex N₃-CL/siRNA was subsequently constructed with the anionic module propiolic acid (PA) *via* the azide/alkyne chemical reaction to obtain the PC. To ensure the linkage of alkyne-terminated anionic molecules to the azide functionalized complex, a model reaction between the cationic lipid (N₃-LG2C₁₄) with an azide group and the PA with an alkynyl group was conducted. The reaction procedure catalysed by the *in situ* generation of active Cu(I) *via* the reduction of CuSO₄ by sodium ascorbate proved to be highly satisfactory and reliable (Scheme S3†). The size and surface potential of the N₃-CL/siRNA complex at different N/P ratios (Fig. S1†) were determined using dynamic light-scattering, and an optimal N/P (4 : 1) ratio was selected since the so-obtained PC satisfactorily exhibited negative charge (−18.7 mV) at pH 7.4 and reversed to positive charge (+9.6 mV) at pH 6.5, which was attributed to the shedding of electronegative PA coatings (Fig. 2a). This PC was further characterized using high resolution transmission electron microscopy (HRTEM), FTIR spectroscopy and ultraviolet spectroscopy. Additionally, the image of the HRTEM examination showed a spheroid structure of the PC with a uniform particle size of about 110 nm (Fig. 2b). The disappearance of the infrared absorption peak of azide at 2101 cm⁻¹ (Fig. S2a†) and the increased ultraviolet absorbance are due to the generation of triazole groups after the reaction between the azido-functionalized complex and PA (Fig. S2b†). No undesirable release and destruction of encapsulated siRNA were detected after the assembly (Fig. 2c). As a control, the cationic liposomes CL without azide modification containing LG2C₁₄ and the complex between CL and siRNA, named CC, were also prepared with a resulting particle diameter of 118.2 nm and a zeta potential of 19.7 mV at a N/P ratio of 4 : 1 (mol : mol) (Fig. S3a†). The encapsulation of siRNA by the CC was also confirmed by the gel electrophoresis assay (Fig. S3b†).

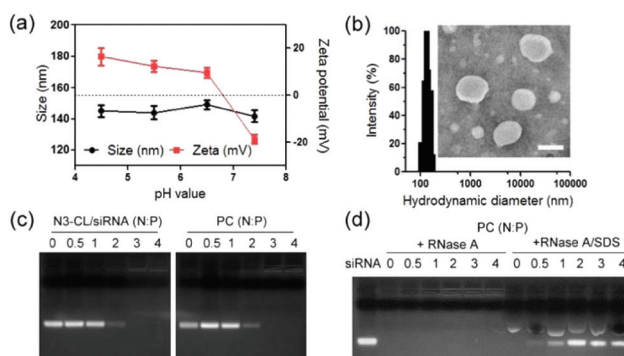


Fig. 2 (a) Particle size and zeta potential of the PC at different pH values (pH 7.4, pH 6.5, pH 5.5, pH 4.5). (b) Size distribution histogram and TEM image of the PC (N : P = 4 : 1, molar ratios). Scale bar indicates 100 nm. (c) Agarose gel electrophoresis analysis of N₃-CL/siRNA and the PC at different N : P ratios. (d) Protection of siRNA against RNase A digestion by the PC under various N : P ratios in the absence or presence of SDS.

It is well known that the complex should protect the siRNA from premature release in a complicated physiological environment before arriving at the destination. In view of this, we evaluated the stability of the PC under different physical circumstances, such as the serum (pH 7.4) and tumor microenvironment (pH 6.5), taking advantage of the fluorescence resonance energy transfer (FRET). Thus, the double-fluorescence labelled PC was prepared with the rhodamine B labelled cationic lipid (RhB-N₃-LG2C₁₄) (Scheme S4†) and FAM labelled siRNA (FAM-siRNA) (1:1, w:w), in which the fluorescence coming from the donors (FAM-siRNA) is substantially reduced (Fig. S4a†). Then, we estimated the integrity of the complex according to the change of the FRET efficiency ($I_{\text{RhB}}/I_{\text{RhB}} + I_{\text{FAM}} \times 100\%$).²⁴ It was shown that the FRET efficiency remained at similar levels over time, revealing that the PC remained stable in the presence of the serum and at different pH values, while an overt reduction was revealed in the CC at pH 7.4 or in the serum (Fig. S4b†). Meanwhile, the particle size of the PC in the presence of the serum or at pH 7.4 and pH 6.5 was determined, which exhibited little change at different time intervals. Note that the CC manifested apparent variations in the serum or at pH 7.4 (Fig. S5†). In addition, since the siRNA tends to be degraded by ribonucleases (such as RNase A) in the body, we evaluated whether the PC could protect siRNA from degradation by RNase A. The result showed that no degradation of the encapsulated siRNA was observed (Fig. 2d).

3.2 Cellular uptake and intracellular distribution of siRNA

For the purpose of evaluating the response towards the acidity of the tumor microenvironment, the cellular uptake of the PC loading FAM-siRNA was determined on human hepatocellular carcinoma cells (Bel-7402) using flow cytometry and confocal laser scanning microscopy (CLSM) (Fig. 3a and Fig. S6†). The cellular uptake of the PC at pH 6.5 was significantly higher than that at pH 7.4, indicating a pH-dependent uptake process of the PC which would selectively enter tumor cells *via* endocytosis. Contrarily, the cellular uptake of the CC was not significantly affected by the changes of the pH values. We also found that the presence of chlorpromazine, the inhibitor of clathrin-mediated endocytotic pathway, and amiloride, the inhibitor of macropinocytosis,³⁰ exerted a distinct effect on inhibiting the

cellular uptake of the PC, implying the endocytosis mediated cell uptake pathways (Fig. S7†). Furthermore, the Bel-7402 cells labelled with LysoTracker were observed by CLSM after incubation with the PC loaded with FAM-siRNA. After 3 h, the fluorescent signal of FAM-siRNA (green) was mainly co-localized with the signal of LysoTracker (red), indicating that the PC was entrapped into the endosome after the uptake by Bel-7402 cells. Nevertheless, after 6 h of incubation, a great signal separation of FAM-siRNA and LysoTracker was observed, confirming the efficient endosomal escape of the PC (Fig. S8†). As is well known, an ideal siRNA delivery system should possess the properties of intelligent disassembly to release siRNA in order to ensure its gene silencing efficiency. To evaluate the disassembly of the PC, the membrane fusion between the PC and isolated endosome/lysosome was investigated under different pH values. It turned out that the PC exhibited the high fusogenic potential at acidic environments (Fig. 3b), but the PC hardly fused with the endosome/lysosome membrane at pH 7.4. Hence, we inferred that the PC could be disassembled and the siRNA released into the cytoplasm *via* the fusion with the endosome/lysosome membrane. To further evaluate the intracellular release of siRNA, the Bel-7402 cells were incubated with the RhB-labeled PC containing FAM-siRNA over time. After 3 h, the signal of FAM-siRNA (green) was mostly overlaid with the signal of RhB (red), while a great dissociation of the FAM and RhB signals was observed after incubation for 6 h, suggesting an efficient intracellular release due to the membrane fusion of the PC and lysosomes (Fig. S9†).

3.3 Gene silencing efficiency *in vitro*

Then, we evaluated the gene silencing efficiency of the PC loaded with siRNA targeting survivin (cpusiRNA2), as survivin is associated with cancer proliferation and the down regulation of survivin expression by cpusiRNA2 can be used for the treatment of cancers, especially hepatoma.³¹ The gene silencing efficiency was evaluated on Bel-7402 cells at three progressive levels: mRNA transcription, protein expression and cell apoptosis. Firstly, the level of survivin mRNA was analysed at pH 7.4 and pH 6.5 by quantitative real-time polymerase chain reaction (qRT-PCR). The PC loaded with cpusiRNA2 significantly reduced the level of mRNA transcription from the survivin gene at pH 6.5 (35.47% down-regulation) compared to that at pH 7.4 (8.77% down-regulation). It is worth noting that the PC loaded with the negative control siRNA (PC/siN.C.) did not show a significant gene silencing effect, implying that nonspecific gene silencing was inexistent (Fig. 4a). In contrast, the CC loaded with cpusiRNA2 showed no noticeable change of the gene silencing efficiency at different pH values (32.30% at pH 7.4 and 37.27% at pH 6.5 down-regulation, respectively) (Fig. 4b). Then, to confirm whether the survivin protein expression was decreased following the reduction in survivin mRNA, the survivin protein expression was detected by western blot analysis. The results showed that the PC loaded with cpusiRNA2 could remarkably knock down survivin protein expression to a low level at pH 6.5, compared with that at pH 7.4 (Fig. S10a†), whereas the PC/siNC did not bring

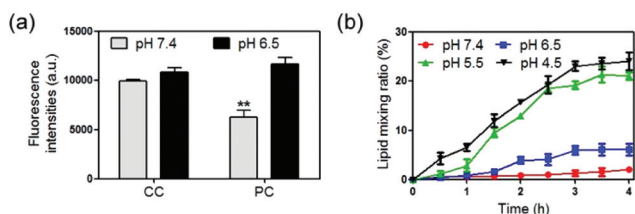


Fig. 3 (a) Cellular uptake of the PC on Bel-7402 cells for 3 h at different pH values identified by flow cytometry. ** $P < 0.01$, compared with that at pH 7.4. (b) Fusogenic potential between the PC and the isolated endosome/lysosomes of Bel-7402 cells as a function of incubation time at different pH values (pH 7.4, pH 6.5, pH 5.5, pH 4.5).

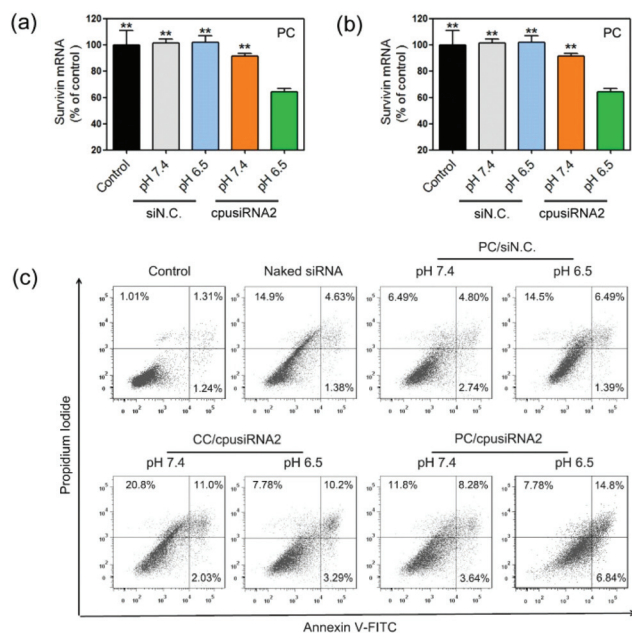


Fig. 4 (a, b) Survivin gene knockdown efficacy in Bel-7402 cells following transfection with the PC and CC at different pH values (pH 7.4 and pH 6.5) determined by qRT-PCR. $**P < 0.01$, compared with that at pH 6.5. (c) Induction of apoptosis on Bel-7402 cells by the CC loaded with cpusiRNA2 and the PC loaded with siN.C. or cpusiRNA2 at different pH values (pH 7.4 and pH 6.5), as well as naked siRNA. Early apoptotic cells are shown in the lower right quadrant, and late apoptotic cells are shown in the upper right quadrant.

about the down-regulation of survivin protein expression at either pH 6.5 or pH 7.4, and the CC loaded with cpusiRNA2 showed little efficiency in the down-regulation of survivin protein expression in Bel-7402 cells at different pH values (Fig. S10b†).

Since the inhibition of survivin expression is associated with the induction of cancer cell apoptosis,³² the enhanced survivin gene silencing efficiency by the PC could promote the apoptosis of Bel-7402 cells. The Bel-7402 cells were stained with a combination of Annexin V-FITC and propidium iodide (PI), and analyzed by flow cytometry (Fig. 4c). The cpusiRNA2 delivered by the PC led to increased cell apoptosis (21.64%) at pH 6.5, compared to that at pH 7.4 (11.92%). Moreover, the CC loaded with cpusiRNA2 show scarce efficiency in the apoptosis-inducing effect of Bel-7402 cells at different pH values. These results demonstrated that the charge reversal of the PC could significantly enhance the target gene silencing efficiency and the consequent biological consequence of anticancer activity.

3.4 Biodistribution, therapeutic efficacy and safety evaluation

Finally, the gene silencing efficiency *in vivo*, tumor targeting ability and anti-tumor efficiency were assessed using ICR mice bearing mice hepatocellular carcinoma (Heps) xenograft tumors. The PC loaded with cpusiRNA2 showed excellent gene silencing efficiency *in vivo* (Fig. 5a and Fig. S11†), in accord-

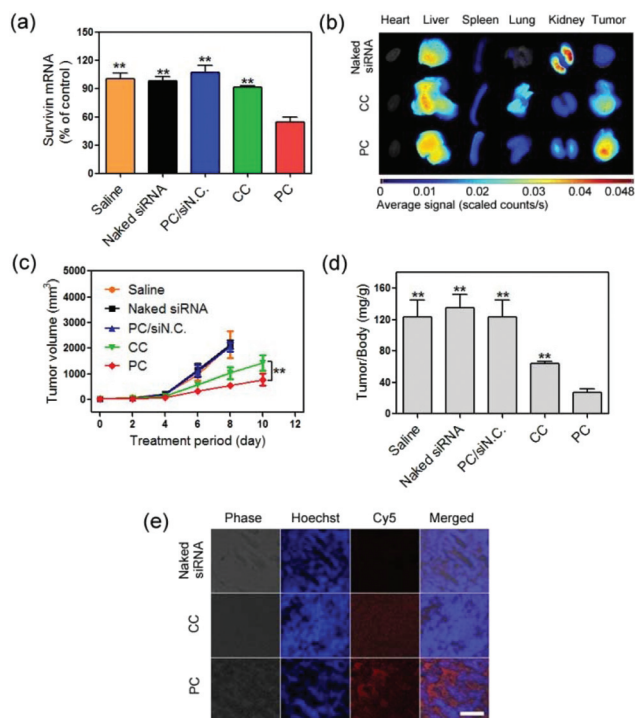


Fig. 5 (a) Survivin gene knockdown efficacy in tumors from the Heps tumor-bearing mice following transfection with different formulations determined by qRT-PCR. $**P < 0.01$, compared with the PC. (b) *Ex vivo* fluorescence imaging of Cy5-labeled siRNA in tumors and normal tissues such as heart, liver, spleen, lung and kidney at 24 h after injection. (c) Tumor growth curves of the Heps tumor-bearing ICR mice subjected to intravenous injection of saline, naked siRNA, PC/siN.C., and CC and PC loaded with cpusiRNA2 at a dose of 1.2 mg kg^{-1} . $**P < 0.01$, compared with the PC. (d) Tumor index of the Heps tumour-bearing ICR mice, calculated by the weight ratio of the tumour to the body, after the treatment with different formulations. $**P < 0.01$, compared with the PC. (e) CLSM images of tumor sections from the Heps tumor-bearing mice at 24 h after intravenous injection of naked Cy5-siRNA, and CC and PC loaded with Cy5-siRNA. Scale bar indicates $50 \mu\text{m}$.

ance with that determined *in vitro*. The biodistribution of the PC encapsulating Cy5-labeled siRNA (Cy5-siRNA) administered intravenously through tail vein injection was observed using a near-infrared imaging technology, compared with naked Cy5-siRNA and the CC (Fig. S12a†). The PC exhibited apparent fluorescence in the tumor area after a short time of injection, higher than that of the CC without an outer anionic layer, possibly due to hemodynamic instability. As time progressed, the elevated tumor fluorescence intensity of the PC was noticeable and remained at a high level until 12 h. In order to quantitatively analyse the biodistribution of Cy5-labeled siRNA, the mice were euthanized to harvest the tumors and normal tissues such as heart, liver, spleen, lung and kidney for *ex vivo* fluorescence imaging at 24 h after injection. The tumor fluorescence intensity of the PC was significantly higher than that of the naked siRNA and the CC (Fig. 5b and S12b†). Meanwhile, the tumor sections harvested from the mice were treated with different formulations after 24 h with the Hoechst

33258-labeled nucleus. As expected, the massive Cy5-siRNA (red) of the PC distributed throughout the tumor section (Fig. 5e). These results implied that the PC could effectively deliver the encapsulated siRNA into the tumor region, facilitating siRNA mediated gene silencing and the consequent antitumor activity. To investigate the antitumor effect of survivin-targeting siRNA delivered by the PC, the inhibition of tumor growth was evaluated following the intravenous injection. Naked siRNA and PC/siN.C. exhibited no apparent anti-tumor efficiency in comparison with saline, and the PC loaded with cpusRNA2 presented obviously higher inhibition efficacy to tumor growth than the CC (Fig. 5c). At the end of the treatment, tumor and normal tissues were harvested and weighed. The mice treated with the PC displayed the lowest mass ratio of the tumor to the body compared to the other formulations, further verifying the enhanced anti-tumor activity of the PC (Fig. 5d).

Meanwhile, the body weight of the mice showed no obvious changes suggesting no apparent toxicity of these formulations during the period of treatment (Fig. S13[†]). Furthermore, the PC loaded with cpusRNA2 brought about no obvious toxicity and cell cycle arrest on normal hepatic cells (Fig. S14[†]). In addition, there is no variation in the caspase gene in normal tissues (data not shown). Therefore, this siRNA delivery system demonstrated a good safety. Histological analysis was carried out with hematoxylin and eosin (HE) staining of the tumor section from the Heps tumor-bearing ICR mice after treatment. Extensive remission of tumor cells and a significant prolongation of the survival period occurred after treatment with the PC, compared to other formulations (Fig. S15 and S16[†]), indicating that the PC was a promising and effective siRNA delivery system for the treatment of Heps tumor-bearing mice.

4. Discussion

In conclusion, we have developed a facile, feasible and efficient assembly strategy to design a tumor targeting siRNA delivery system, which has a tumor acidity-responsive isoelectric point *via* adjusting the ratios of positively and negatively charged modules. The siRNA delivery system composed of different modules can intelligently respond to the acidic microenvironment of the tumor tissue, which is beneficial for cellular uptake, accompanied by enhanced gene silencing efficiency and consequent antitumor therapeutic efficacy. Accordingly, this modular assembly strategy would provide a promising platform for the design of smart siRNA delivery systems with reduced unsatisfied side effects, high targeting efficiency and enhanced therapeutic effects for cancer therapy.

Conflicts of interest

There are no conflicts to declare.

Acknowledgements

This work was supported by the National Natural Science Foundation of China (81773664, 81473153), the National Basic Research Program of China (2015CB755504), the 111 Project from the Ministry of Education of China and the State Administration of Foreign Expert Affairs of China (No. 111-2-07). The authors thank the public platform of the State Key Laboratory of Natural Medicines for assistance with confocal microscopy and flow cytometry.

Notes and references

- 1 C. Morrison, *Nat. Rev. Drug Discovery*, 2018, **17**, 156–157.
- 2 S. A. Gorski, J. Vogel and J. A. Doudna, *Nat. Rev. Mol. Cell Biol.*, 2017, **18**, 215–228.
- 3 W. Z. Liao, W. Li, T. T. Zhang, M. Kirberger, J. Liu, P. Wang, W. Chen and Y. Wang, *Biomater. Sci.*, 2016, **4**, 1051–1061.
- 4 E. Keles, Y. Song, D. Du, W. J. Dong and Y. H. Lin, *Biomater. Sci.*, 2016, **4**, 1291–1309.
- 5 Y. H. Roh, J. Z. Deng, E. C. Dreaden, J. H. Park, D. S. Yun, K. E. Shopsowitz and P. T. Hammond, *Angew. Chem., Int. Ed.*, 2016, **55**, 3347–3351.
- 6 E. J. Lee, S. J. Lee, Y. S. Kang, J. H. Ryu, K. C. Kwon, E. Jo, J. Y. Yhee, I. C. Kwon, K. Kim and J. Lee, *Adv. Funct. Mater.*, 2015, **25**, 1279–1286.
- 7 M. Rezaee, R. K. Oskuee, H. Nassirli and B. Malaekhe-Nikouei, *J. Controlled Release*, 2016, **236**, 1–14.
- 8 X. X. Liu, C. Liu, J. H. Zhou, C. Chen, F. Q. Qu, J. J. Rossi, P. Rocchi and L. Peng, *Nanoscale*, 2015, **7**, 3867–3875.
- 9 X. J. Loh, T. C. Lee, Q. Q. Dou and G. R. Deen, *Biomater. Sci.*, 2016, **4**, 70–86.
- 10 H. Yin, R. L. Kanasty, A. A. Eltoukhy, A. J. Vegas, J. R. Dorkin and D. G. Anderson, *Nat. Rev. Genet.*, 2014, **15**, 541–555.
- 11 C. N. Xu, H. Y. Tian, P. Wang, Y. B. Wang and X. S. Chen, *Biomater. Sci.*, 2016, **4**, 1646–1654.
- 12 Y. Liu, G. Zhao, C. F. Xu, Y. L. Luo, Z. D. Lu and J. Wang, *Biomater. Sci.*, 2018, **6**, 1592–1603.
- 13 G. M. Lin, C. B. Yang, R. Hu, C. K. Chen, W. C. Law, T. Anderson, B. T. Zhang, Q. T. Nguyen, H. T. Toh, H. S. Yoon, C. Cheng and K. T. Yong, *Biomater. Sci.*, 2014, **2**, 1007–1015.
- 14 S. J. Lee, M. J. Kim, I. C. Kwon and T. M. Roberts, *Adv. Drug Delivery Rev.*, 2016, **104**, 2–15.
- 15 F. Ding, Q. B. Mou, Y. Ma, G. F. Pan, Y. Y. Guo, G. S. Tong, C. H. J. Choi, X. Y. Zhu and C. Zhang, *Angew. Chem., Int. Ed.*, 2018, **57**, 3064–3068.
- 16 H. Takemoto, K. Miyata, S. Hattori, T. Ishii, T. Suma, S. Uchida, N. Nishiyama and K. Kataoka, *Angew. Chem., Int. Ed.*, 2013, **52**, 6218–6221.
- 17 X. D. Xu, J. Wu, Y. L. Liu, M. Y. Yu, L. L. Zhao, X. Zhu, S. Bhasin, Q. Li, E. Ha, J. J. Shi and O. C. Farokhzad, *Angew. Chem., Int. Ed.*, 2016, **55**, 7091–7094.

- 18 H. J. Kim, A. Kim, K. Miyata and K. Kataoka, *Adv. Drug Delivery Rev.*, 2016, **104**, 61–77.
- 19 S. Tang, Q. S. Meng, H. P. Sun, J. H. Su, Q. Yin, Z. W. Zhang, H. J. Yu, L. L. Chen, Y. Chen, W. W. Gu and Y. P. Li, *Adv. Funct. Mater.*, 2016, **26**, 6033–6046.
- 20 X. W. Guan, Z. P. Guo, L. Lin, J. Chen, H. Y. Tian and X. S. Chen, *Nano Lett.*, 2016, **16**, 6823–6831.
- 21 Q. Sun, Z. S. Kang, L. J. Xue, Y. K. Shang, Z. G. Su, H. B. Sun, Q. N. Ping, R. Mo and C. Zhang, *J. Am. Chem. Soc.*, 2015, **137**, 6000–6010.
- 22 S. J. Tseng, Z. X. Liao, S. H. Kao, Y. F. Zeng, K. Y. Huang, H. J. Li, C. L. Yang, Y. F. Deng, C. F. Huang, S. C. Yang, P. C. Yang and I. M. Kempson, *Nat. Commun.*, 2015, **6**, 6456.
- 23 C. Y. Ju, R. Mo, J. W. Xue, L. Zhang, Z. K. Zhao, L. J. Xue, Q. N. Ping and C. Zhang, *Angew. Chem., Int. Ed.*, 2014, **53**, 6253–6258.
- 24 Y. P. Li, W. W. Xiao, K. Xiao, L. Berti, J. T. Luo, H. P. Tseng, G. Fung and K. S. Lam, *Angew. Chem., Int. Ed.*, 2012, **51**, 2864–2869.
- 25 Y. Obata, D. Suzuki and S. Takeoka, *Bioconjugate Chem.*, 2008, **19**, 1055–1063.
- 26 X. X. Zhang, P. G. Allen and M. Grinstaff, *Mol. Pharmaceutics*, 2011, **8**, 758–766.
- 27 E. Dudleenamjil, C. Y. Lin, D. Dredge, B. K. Murray, R. A. Robison and F. B. Johnson, *J. Gen. Virol.*, 2010, **91**, 3032–3041.
- 28 M. Koivusalo, C. Welch, H. Hayashi, C. C. Scott, M. Kim, T. Alexander, N. Touret, K. M. Hahn and S. Grinstein, *J. Cell Biol.*, 2010, **189**, 385.
- 29 F. Fazlollahi, S. Angelow, N. R. Yacobi, R. Marchelletta, A. S. Yu, S. F. Hamm-Alvarez, Z. Borok, K. J. Kim and E. D. Crandall, *Nanomedicine*, 2011, **7**, 588–594.
- 30 R. Mo, Q. Sun, J. W. Xue, N. Li, W. Y. Li, C. Zhang and Q. N. Ping, *Adv. Mater.*, 2012, **24**, 3659–3665.
- 31 Y. H. Lu, K. Wang, R. He and T. Xi, *Cancer Biother. Radiopharm.*, 2008, **23**, 727–733.
- 32 D. H. Park, J. Cho, O. J. Kwon, C. O. Yun and J. H. Choy, *Angew. Chem., Int. Ed.*, 2016, **55**, 4582–4586.